**Ferroudja BOUALI[1], Hassane MOHELLEBI[1], Ghania YOUSFI[1]**

Department of Electrotechnics, Mouloud Mammeri University of Tizi Ouzou, Algeria (1)

doi:10.15199/48.2021.03.21

# Coupled Circuit Method Applied to the detection of Defects in a Conductive Multilayer Device

***Abstract***. *The work present the coupled circuit method applied to an eddy current nondestructive testing (EC-NDT) problems. The device is consisting on a conductive multilayer structure having an air gap (delamination), or a physical defect (lack of material). The purpose of the study is to identify the presence of the delamination when a physical defect can occur simultaneously. The use of Coupled Circuits Method permits to reduce the discretization to only the active parts without mesh air gap. The results obtained are compared to finite elements ones. A good agreement is observed between results. Interesting and useful conclusions are made.*

***Streszczenie.*** *W pracy przedstawiono metodę obwodów sprzężonych zastosowaną do badań nieniszczących prądów wirowych (EC-NDT). Urządzenie składa się z przewodzącej konstrukcji ze szczeliną powietrzną (rozwarstwieniem) lub wadą fizyczną (brak materiału). Celem badania jest identyfikacja obecności rozwarstwienia, gdy jednocześnie może wystąpić wada fizyczna. Zastosowanie metody obwodów sprzężonych pozwala zredukować dyskretyzację tylko do aktywnych części bez siatkowej szczeliny powietrznej. Uzyskane wyniki porównuje się z wynikami elementów skończonych. Obserwuje się dobrą zgodność wyników. (**Zastosowanie metody obwodów sprzężonych do detekcji defektów w materiałach przewodzących**)*

**Keywords:** Coupled circuits method, *Multilayer device, Air gap, Delamination, Defect detection*.
**Słowa kluczowe:** Metoda obwodów sprzężonych, Urządzenie wielowarstwowe, Szczelina powietrzna, rozwarstwiania, Wykrywanie defektów.

## Introduction

The eddy current testing is used in all types of industries using parts of electrically conductive material, particularly metallurgy, nuclear power, petrochemicals, railways, aerospace, armaments, industry shipbuilding, automotive and aerospace.

This popularity and diversity are due to technical features including simplicity, the implementation of complex structures with adaptable sensors, portable equipment, high sensitivity, non-necessity of contact with the target, real-time response, the ability to automate the testing and analysis of test results [1] with aging, had become sensitive to cyclic fatigue defects in multilayer structures [2,3]. In addition, delamination between the different layers is one of the observed damage modes [4,5,6], the propagation of one or the other causes the inevitable rupture.

In The semi-analytical formulations based on integral equations realize an interesting compromise between accuracy and computational time which results in a relatively reduced calculation time. In this work we are interested in the method of electric coupled circuits developped and applied to several devices [7,8, 9,10,11,12]. Based on the calculation of mutual inductances, this method has the advantage of discretizing the actives parts and thus the advantage of do not meshes air region and mainly fine gap layer. Others semi-analytical solutions use either a magnetic vector potential as unknown variable when applying coupled circuits method [12] or a solution of partial differential equations in its 2D or 3D forms [13,14,15].

The most previous works in NDT consider a monolayer structure; some ones use an hybrid method with the association of coupled circuit method in an optimization procedure when a delamination occurs in the multi-layer plate[16]. A stratified metallic cylinder is also studied for mechanical stress evaluation [16,6].

The aim in this work is to detect and identify the presence of delamination separating the conductive layers simultaneously when a physical defect (lack of material) exists in the structure [2,3,5,6].

The geometry of the survey system is represented by Fig.1. The three-dimensional model is reduced to a two-dimensional one in the study by considering an axisymmetric physical problem.

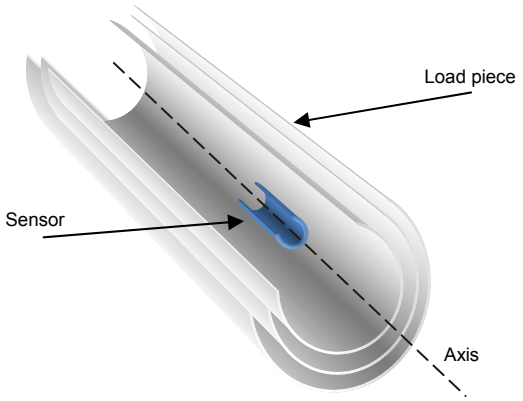


Fig. 1. Structure of the study device

## Coupled Circuits Method

The method of coupled circuits operates a calculus for assessing the electrical parameters of the system from the mutual inductances. This process makes it possible to express the self-inductance, the resistance of each elementary coil and mutual inductances between coils. The resistance $R_i$ of the elementary turns $i$ is obtained using analytical formula. Terms that allow the calculation of the latter are given by equations (1) (2) and (3) below [17,18] respectively:

$$R_i = \rho \frac{l_i}{S_i} \tag{1}$$

$$l_i = 2\pi r_{ai} \tag{2}$$

$\rho_i$: electrical resistivity, $S_i$: cross section of elementary section, $r_{ai}$: average radius of the elementary coil.

In the this study, we consider that the mutual inductance $m_{ij}$ between two elementary coils $i$ and $j$, assumed to be filaments elementary coils, is given by [18]:

$$M_{ij} = \frac{1}{n^2} \sum_{i=1}^{n} \sum_{\substack{j=1 \\ j \neq i}}^{n} m_{ij} \tag{3}$$

(4) $$m_{ij} = \mu_0 \sqrt{r_i r_j}\left[\left(\frac{2}{k} - k\right)k(k) - \frac{2}{k}E(k)\right]$$

(5) $$k^2 = \frac{4\, r_i\, r_j}{(r_i + r_j) + h^2}$$

The total inductance $L_{ij}$ between elementary coils *i* and *j* of the conducting ring is obtained by expression (6):

(6) $$L_{ij} = \frac{1}{n^2}\sum_{i=1}^{n}\sum_{\substack{j=1 \\ j\neq i}}^{n} m_{ij} + \frac{1}{n}\sum_{i=1}^{n} L_{p_i}$$

$\mu_0$: magnetic permeability of vacuum, $r_i$ : radius of the elementary coil *i*, $r_j$ : radius of the turn *j*, *h*: distance between the two elementary coils, *K(k)* et *E(k)*: elliptic integrals, *r* : radius of the copper conductor.

The self-inductance is given by the formula (7):

(7) $$L_{pi} = \mu_0\, a\left(\ln\left(\frac{8\,a}{r} - 1.75\right)\right)$$

The well known Kirchhoff's laws are applied to the equivalent electrical circuit of the non-destructive testing device, having a tube with conducting layers (two and three) and a sensor of 140 turns, given in Fig. 3, allow us to obtain the associated electrical equations for each filament m and n as following:

(8) $$U_{b_i} = R_{b_i}\, I_{b_i} + j\omega L_{b_i}\, I_{b_i} + j\omega \sum_{\substack{b'_i=1 \\ b'_i\neq b_i}}^{m} M_{b_i b'_i}\, I_{b'_i} + j\omega \sum_{c_{1j}=1}^{n} M_{c_{1j} b_i}\, I_{c_{1j}} + j\omega \sum_{c_{2j}=1}^{n} M_{c_{2j} b_i}\, I_{c_{2j}}$$

(9) $$0 = R_{c_{1j}}\, I_{c_{1j}} + j\omega L_{c_{1j}}\, I_{c_{j1}} + j\omega \sum_{\substack{c'_{1j}=1 \\ c'_{1j}\neq c_{1j}}}^{n} M_{c_{1j} c'_{1j}}\, I_{c'_{1j}} + j\omega \sum_{c_{2j}=1}^{n} M_{c_{1j} c_{2j}}\, I_{c_{2j}} + j\omega \sum_{b_i=1}^{m} M_{c_{1j} b_i}\, I_{b_i}$$

The geometry of the studied problem concerns a 2D axisymmetric structure considered in (r, z) coordinates as shown in the following Fig. 2:

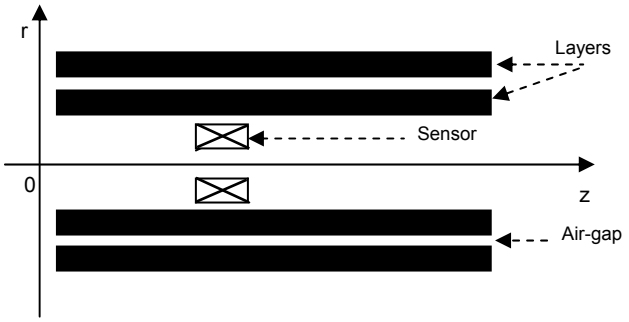


Fig. 2. Representation in the (r, z) plane of the NDT device

The equivalent electrical circuit considered for the current study device when the inductor is divided into m elementary turns and the load piece (the two and three layers) into n elementary turns respectively is represented by Fig. 3. In this study the inductor is assumed to be a one coil with : 0.75 mm x 0.75 mm section and then divided to n elementary turns [10].

Note that electrical equivalent circuits of conducting layers representing the load piece with the air-gap are short-circuited.

(10) $$0 = R_{c_{2j}}\, I_{c_{2j}} + j\omega L_{c_{2j}}\, I_{c_{2j}} + j\omega \sum_{\substack{c'_{2j}=1 \\ c'_{2j}\neq c_{2j}}}^{n} M_{c_{2j} c'_{2j}}\, I_{c'_{2j}} + j\omega \sum_{c_{1j}=1}^{n} M_{c_{1j} c_{2j}}\, I_{c_{j1}} + j\omega \sum_{b_i=1}^{m} M_{c_{2j} b_i}\, I_{b_i}$$

Knowing that: $R_{c1}$, $R_{c2}$, $R_b$, $L_{c1}$, $L_{c2}$, $L_b$, $I_{c1}$, $I_{c2}$, $I_b$: are resistances, self-inductances and electrical currents of layer 1, layer 2 and inductor coil elements respectively. The mutual inductance coefficients $M_{c1c1}$, $M_{c2c2}$, $M_{bb}$, $M_{c1c2}$, $M_{c1b}$, $M_{c2b}$ determine the influence between layer 1 (index $c_1$), layer 2 (index $c_2$) and inductor coil (index b) respectively when $U_{bi}$ represents the supply voltage.

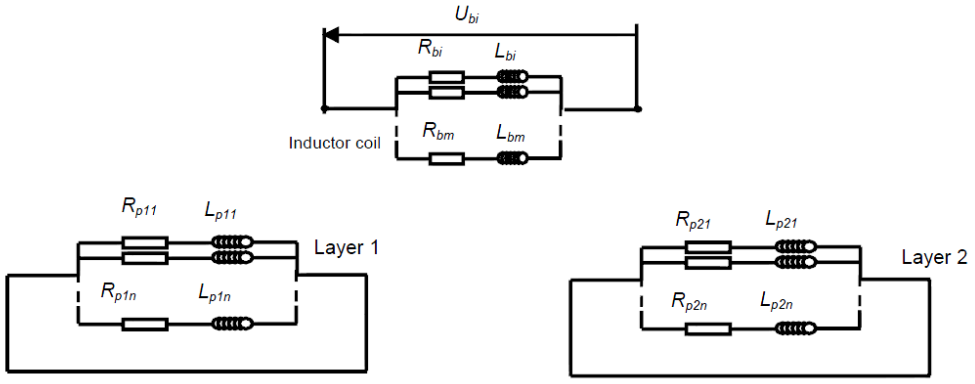


Fig. 3. Electrical equivalent circuit representing the sensor and 2 layers of conducting load

**The algebraic matrix system**

When writing the electrical equation for the set of elementary turns of the complete device (sensor and layers), the algebraic matrix system obtained has the form bellow:

(11) $$([M] + j\omega[\mathrm{N}])[I] = [\mathrm{K}]$$

(12) $$\omega = 2\pi f$$

$f$ is the frequency, $[I]$ is the unknown vector which represents the electrical currents of elementary turns with dimension (2*n + m). The second term in equation (11) contain the source terms of dimension (2*n + m) with n non zeros source terms. The self-inductance and the mutual inductance of each elementary turn are given in the square matrix [*N*] of dimensions (2*n + m) x (2*n + m); $[M]$ is square matrix which terms are the resistances of elementary turns.

**Application and results**

The geometry represented in Fig. 2 is discretized to elementary turns (inductor: 24 elementary coils, layer tube: 30x10 elementary coils), as its symmetry only a half part of the 2D geometrical model is considered. The geometry shown in Fig. 4 is consisting of a half part of a cylindrical two layers structure having a defect at the outer layer and an air-gap representing the delamination. The effect of the delamination or the physical defect (lack of material) or both them on the non-destructive testing study in cases of two layers at first and three layers later, is investigated.

**Non Destructive Testing Study of a Two Layers Cylindrical Tube**

The resolution domain for the sensor-load system is represented by Fig. 4. The physical and geometrical characteristics of NDT system are given in Table 1.

*Table 1. Physical and Geometrical Parameters*

| Physical and Geometrical Parameters | Sensor | Conducting Layer 1 | Conducting Layer 2 | Defect |
|---|---|---|---|---|
| Length [m] | $0.75*10^{-3}$ | $60*10^{-3}$ | $60*10^{-3}$ | $6*10^{-3}$ |
| Thickness [m] | $0.75*10^{-3}$ | $0.6*10^{-3}$ | $0.6*10^{-3}$ | $0.3*10^{-3}$ |
| Inner radius [m] | $0.5*10^{-3}$ | $1.3*10^{-3}$ | $1.9*10^{-3}$ | - |
| Magnetic Permeability [H/m] | $4\pi*10^{-7}$ | $4\pi*10^{-7}$ | $4\pi*10^{-7}$ | - |
| Electrical Resistivity [Ω.m] | $1.79*10^{-9}$ | $2.62*10^{-8}$ | $2.62*10^{-8}$ | - |

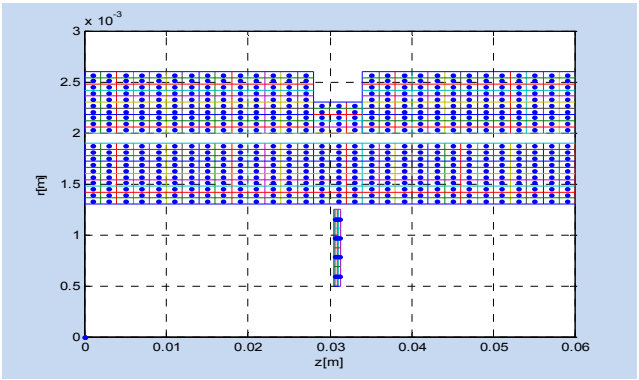


Fig. 4: Discretization of resolution domain (Half device)

**Detection of the air gap (Delamination) Between Two Layers Cylindrical Tube**

The study of the detection of the air gap between two layers in cylindrical tube is conducted by computing the variation of the difference impedance $\Delta Z = |Z - Z_0|$. It is obtained by calculating the difference between the impedance Z of the sensor, including the two layers cylindrical tube, with the presence of the simulated constant air gap and the one obtained when the two layers cylindrical tube are considered without presence of the air gap (called $Z_0$).

At the first step, the study concerns the two layers cylindrical tube having an air-gap between the layers but without physical defect (lack of material). The scan is realized by moving the sensor at the inner tube, the difference impedance ΔZ is then computed for each position (total number of computed positions is 40). This operation is repeated for three value of the air-gap (0.1 mm, 0.2 mm, 0.3 mm) and the results are presented in Fig. 5.

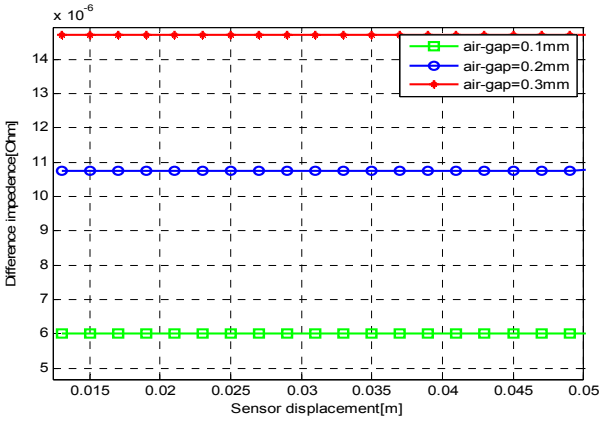


Fig. 5 : Difference impedance ΔZ variation versus the displacement "z" for three values of the air-gap width

The results obtained and given in Fig.5 show that, for a constant thickness of the air-gap, the difference impedance gives a same value for all sensor displacements and its amplitude grows when the air-gap becomes higher. This allows us to an easy detection of the presence of an air gap defect (delamination) in the conducting multilayer's tubes.

**Defect Detection on a Two Layers Cylindrical Tube**

In the current section we consider the two layers conducting tube which contain a defect realised at the outer layer of the conducting tube. The defect has a thickness of 0.3 mm with 6 mm of length. The inspected tube is considered with no presence of air gap (delamination).

In Fig. 6 is shown the evolution of the difference impedance ΔZ when the position of the sensor change along the z direction (Fig. 6).

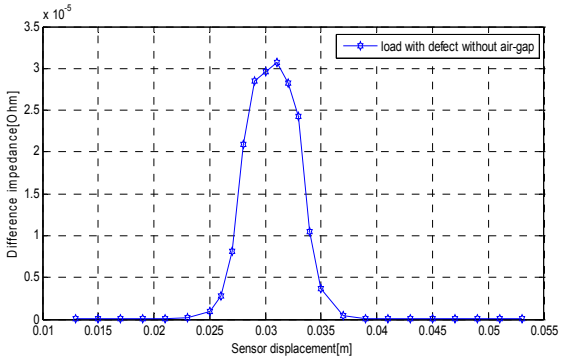


Fig. 6 : Difference impedance behavior ΔZ according to sensodisplacement along z coordinate

The results given in Fig. 6 show a variation of difference impedance $\Delta Z$ from z=0.0023 m to z=0.038 m which variation correspond to the defect position in the conducting two layers tube. The response of the sensor signal, by computing the difference impedance $\Delta Z = |Z - Z_0|$, in case of defect zone or delamination (air-gap) allows quick recognition of the nature of the abnormality holding account of the parabolic shape of the signal obtained when the abnormality is a fault corresponding to a lack of material. For a delamination fault the obtained signal is a constant amplitude level.

**Defects Detection of Simultaneous Abnormalities on a Two Layers Cylindrical Tube**

Studying the possibility that the part to be inspected can have both types of defects , namely a lack of material and air gap inclusion (delamination), is necessary in order to achieve characterize each type of anomaly by the analyze of the response of the sensor signal corresponding to a difference impedance variation according to sensor position.

Thus, the multilayer conductive tube inspected in this case includes a groove on the outer layer of the load and an air gap between the two conductive layers of the tube. The dimensions of the groove are identical to those of the problem discussed above. The air gap represented by a constant thickness between the two layers was taken successively equal to: 0.1 mm, 0.2 mm and 0.3 mm.

The results without presence of air gap defect are added and represented in the same graph shown by Fig. 7.

It is noted that the difference impedance reaches its maximum value in the defect zone and its value increase as the thickness of the air gap increases. Against, by the impedance does not vanish, outside the defect area but tends towards a constant value whose magnitude depends on the thickness of the air gap layer.

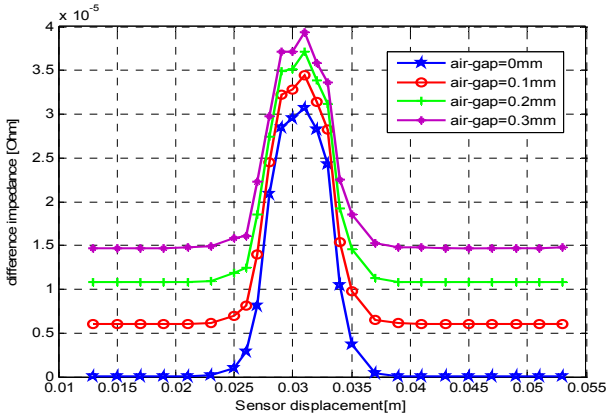


Fig. 7: Evolution of the difference impedance $\Delta Z$ according to sensor position for different values of air-gap thickness

The simulations realized when considering different cases of abnormalities occurring on the conducting multilayer load piece: a flawless load with air-gap, a load with defect represented by a lack of material without inclusion of air-gap and finally a simultaneously presence of a lack of material and an air-gap are summarized and shown in Fig. 8.

One notices that the sensor difference impedance for a load simultaneously presenting defects of a lack of material and an air-gap is predominant, held account of the cumulative effects of the defect and the air-gap presence, the first modifies the currents trajectory and the second reinforces the reluctance value which reduces the magnetic flux and consequently the magnetic flux density. Finally the difference impedance computed becomes higher because of the inverse proportionality variation of the inductance.

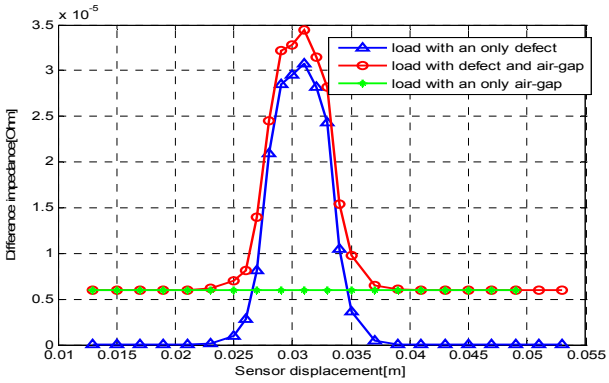


Fig. 8: Evolution of the difference impedance $\Delta Z$ according to sensor position for different abnormalities in the load

**Comparison with numerical calculation**

The comparison of the obtained results using circuits coupled method, based on the use of the mutual inductances computation approach, with the results given when the resolution method chosen is finite elements one are given for 2D axisymmetric solution in the following Fig 9.

The results represented in Fig. 9 are relative's values. The results are reproduced correctly by finite element model. The difference appears at the corners zones of defect due to finite elements mesh quality.

The coupled circuits solution do not induces oscillations comparing to finite element solution. Difference can be reduced by improvement of the finite element mesh around the edges of defect and the air-gap. The validity of the coupled circuits Model is cheeked.

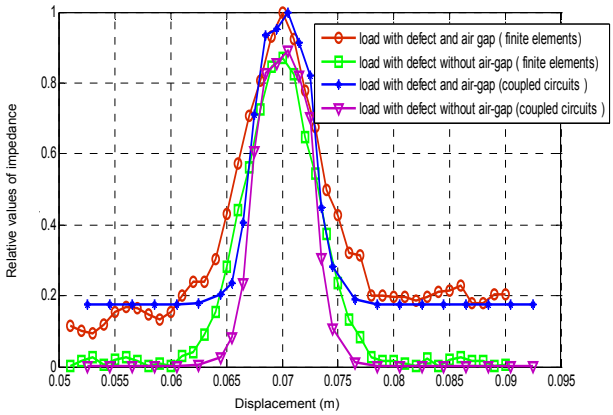


Fig. 9. Confrontation results: coupled circuits and finite elements methods

**Non Destructive Testing Study of a Three Layers Cylindrical Tube**

**Study of the effects of air-gap and lack of material**

In this section we are interested in a conducting multilayer load presenting three identical layers (Fig.10). The considered survey consists in fixing the sensor position and proceeds to the thickness variation of the air-gap zone situated between the conductive layers of the load. For each value of the air-gap one recovers the corresponding value of the sensor impedance (Fig. 11, Fig. 12).

In Fig. 11 are represented the values of the difference impedance $\Delta Z$ obtained for each value of the air-gap layer's thickness. The results are obtained for values of the air-gap thickness varying between 15 $\mu$m and 300 $\mu$m.

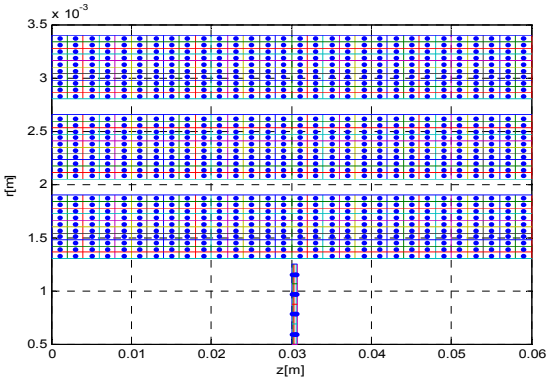


Fig. 10. Representation of healthy solving domain

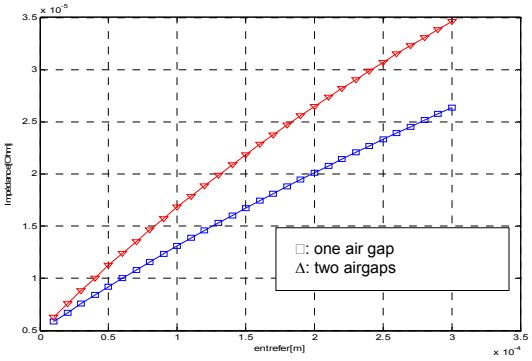


Fig.11. Evolution of ΔZ with the air-gap layer's thickness variation

It is noted that ΔZ value increases when the air-gap thickness increases. The impedance variation computed permits an analysis of the load structure that would lead to deduce the number of air-gaps inclusion in layers in the stratified load, as the results show a significant difference between a load comprising only one air-gap inclusion in layers and those with two air-gaps inclusions in layers (Fig. 11). The importance of the defect represented by the air gap (delamination) could be highlighted by analyzing the magnitude of the difference impedance ΔZ.

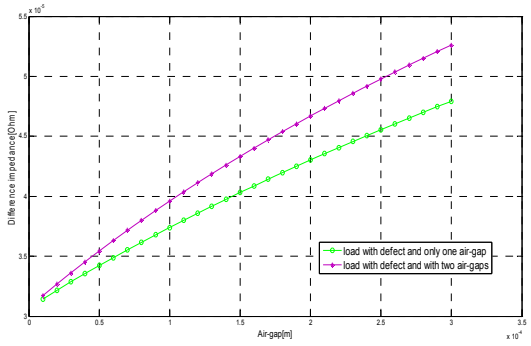


Fig. 12. Evolution of ΔZ value for different values of the air-gap layer's thickness

In Fig. 12 are shown the results corresponding to multilayer conductive load having a lack of material. The sensor positioned and is adjusted to z=0.03 m corresponding to the maximum impedance value for the vicinity of the defect center.

The same behavior could be note comparing with the healthy multilayer conductive load. But in this case the amplitude of the difference impedance is more important and then the abnormality is easily detectable. It could be also defined a range of abnormality nature or characterize the defect nature according to difference impedance ΔZ level obtained. In Fig. 13 are given the results obtained for the different nature of defects considered occurring in case of a healthy body, a physical defect (lack of material) and by inserting one or two air-gaps layers, according to the air gap thickness variation.

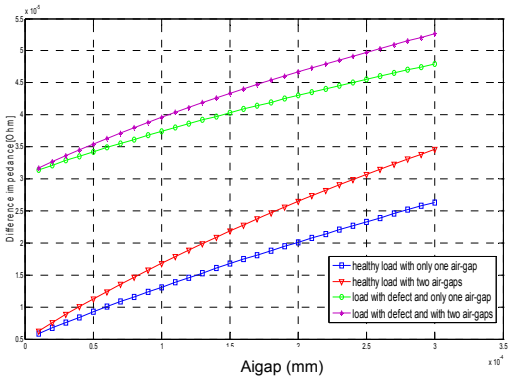


Fig. 13. Evolution of ΔZ value for healthy load and a load having a lack of material as defect

One notices that impedance corresponding to a load including a defect (lack of material) and two air gaps is major (Fig.13). One also notes that the defect presence of 300 μm in a conductive layer with a delamination of 10 μm makes invisible the delamination anomalies whose thickness is lower than 300 μm (Fig. 13).

The sensor impedance corresponding to a load including a lack of material and two air gaps layers is superior to that of a load with lack of material and having a single air-gap layer. When the delamination zone has an important thickness, the sensitivity of the sensor to the presence of two air gaps zones is better (Fig. 11, Fig. 12).

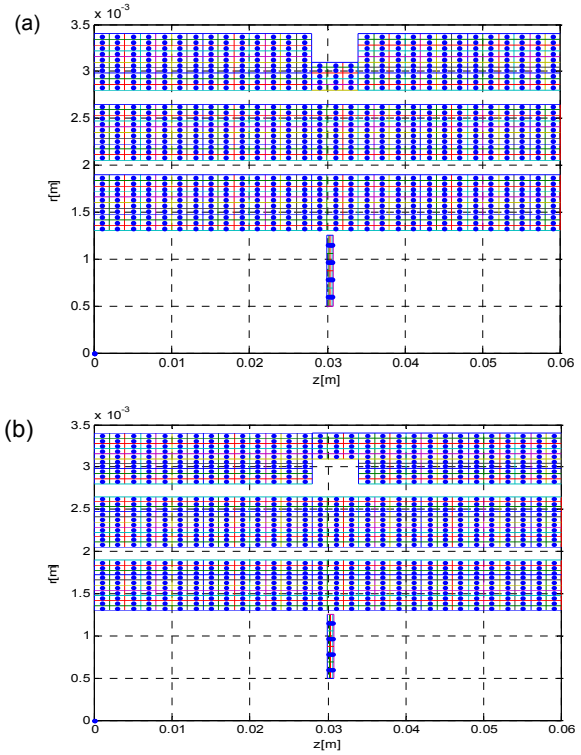


Fig. 14. Solving domain with external and internal defects

**Load presenting internal and external defects Variation of the air-gap layer's thickness**

In this case, one inserts an external defect of 300 μm of thickness and 6 mm of length in one of the conductive

layers of the load presenting a single air-gap layer at first and then two air gaps layers (Fig.14. a) for the second steps. An internal defect of same dimensions (300 μm of thickness and 6 mm of length) has been inserted in one of the conductive layers of the load (Fig.14. b) for further analysis.

The results obtained in terms of difference impedance ΔZ value according to the air gap thickness changes are given in the following Fig. 15.

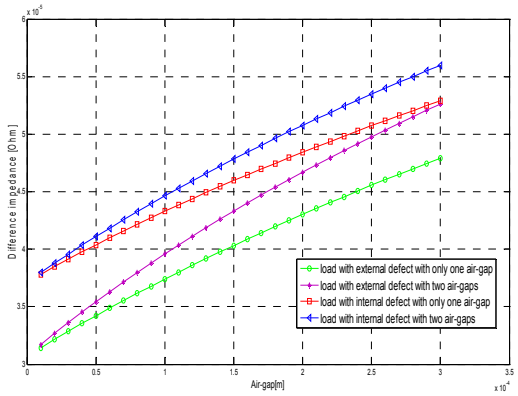


Fig. 15. Evolution of ΔZ impedance value according to the air-gap thickness changes for internal and external defects

From Fig.15 we can see that the internal defect (lack of material) allows to easily detection of the abnormality because of the importance of difference impedance ΔZ parameter. We notice that the internal defect is detected more. Indeed, the ΔZ amplitude is greater than that obtained in the case of the external defect since it is closest to the sensor (Fig. 15). The ΔZ parameter does also increase with the increase of the number of air gaps layers representing the delamination.

In Fig. 16 are given the results in percent related to the difference impedance for the case of a load with two airgaps (the two air gaps have the same thickness) and the load with simultaneously occurring two air gaps and a lack of material (defect). In the second case when the defect is present we could note that the difference impedance present an important gap regarding to the case of only the delamination exist in the load piece. This results appears clearly in Fig. 16 where is presented the difference between the impedances $Z_{airgap}$ (corresponding to the impedance of the load with two defects) and $Z_{airgap+defect}$ (corresponding to the impedance of the load with two air gaps and a lack of material).

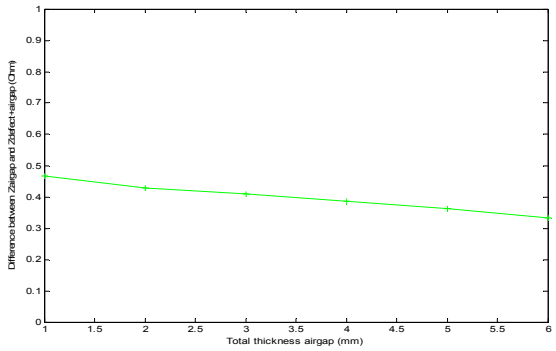


Fig. 17. Evolution of the difference between impedance values according to the total air-gap thickness changes

This result obtained seems to highlight the delamination when operating an inspection of multilayer load as its effect could be detected by computing the relative value of the air gap impedance. In Fig. 17 is presented the result concerning the difference between two values of the impedance corresponding to the two cases presented in Fig. 16. The total air gap represents the air gaps occurring between the three layers (two air gaps).

***Effect of the defect thickness variation***

In order to study the effect of the defect thickness change which is consisting of lack of material defect type one fixes the corresponding thickness to each air gap layer and one achieves a variation of the defect thickness (100 μm, 200 μm, 300 μm) for a fixed sensor position (to the defect center vicinity z=0.03 m). Figure 18 represents the evolution of the difference impedance ΔZ according to the different values considered of the defect thickness.

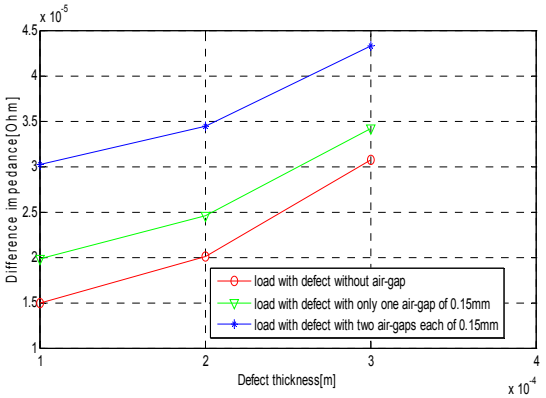


Fig. 18. Evolution of the difference impedance ΔZ with defect thickness change (for different air gap defect)

The ΔZ parameter provided increases when the thickness of the defect increases, which consequently increases the sensor sensitivity. Figure 18 also shows that a delamination on two layers (2x150 μm) and a physical defect of 100 μm makes transparent (invisible) a defect of 300 μm without delamination. In this case the characterization of the anomaly nature must be subject to a further analysis.

**Conclusion**

In this work we have implemented a Half-analytical method called'' Coupled Circuits Method'' based on the evaluation of mutual inductances under MATLAB environment that has the advantage of not discretizing non-conductive regions (air, air gap) and offers an intrinsic precision to the model. Multilayer structures were treated (2 and 3) for non-destructive testing using eddy currents to put in evidence the presence of an air gap (delamination) which is not masked by the defect presence. Thus, the Coupled Circuits Method allows not mesh the delamination zone which is often thin thickness. Numerical methods as finite elements presents some difficulties in modeling thin thickness. The gotten results permit to separate the influence of an air gap (delamination) with that of a defect on the sensor response. A confrontation with a finite element analysis was achieved. The presence of an air gap generates a nearly constant impedance variation whereas the one of a defect produces a peak of the impedance variation in the defect zone. The simultaneous presence of air gaps (delamination) and a defect as lack of material drives to a cumulative of the two effects in the sensor response. In this case further analysis is recommended in order to separate the effects of delamination and those from a material defects. The results obtained allow giving the first answers to the understanding of the effects associated with each phenomenon.

***Authors**: PhD student. Ferroudja Bouali, Department of Electrotechnics, Mouloud Mammeri University of Tizi-Ouzou, BP 17RP 15000, Algeria, E-mail:fer.bouali@yahoo.fr, prof. dr. Hassane Mohellebi, Department of Electrotechnics, Mouloud Mammeri University of Tizi-Ouzou, BP 17RP 15000, Algeria, E-mail: mohellebi@yahoo.fr; PhD student. Ghania Yousfi, Department of Electrotechnics, Mouloud Mammeri University of Tizi-Ouzou, BP 17RP 15000, Algeria, E-mail:ghaniaeth@yahoo.fr.*

## REFERENCES

[1] Abrantes R., Rosado LS., Ramos PM., Piedade M., Embedded Measurement System for Non-Destructive Testing Using New Eddy Currents Planar Array Probe. *IEEE. Transactions On Magnetics* (2014), pp. 583 – 589.

[2] Davis P., Chauchot P., Composites for Marine Applications-Part 2: Underwater Structures, Mechanics of Composites Materials and Structures, Kluwer Academic Publishing (1999), pp. 249-260.

[3] Lifchitz J. M, Dayan H., Filament-Wound Pressure Vessel With Thick Metal Liner, Composites Structures, 32 (1995), pp. 313-323.

[4] Idriss M., El Mahi A., El Guerjouma R., Etude du comportement en statique et en fatigue cyclique d'un matériau sandwich endommagé par décohésion. *20ème Congrès Français de Mécanique*, Besançon, 29 Août au 2 Septembre, (2011).

[5] Stot C. A., Ross Underhill P., Babbar V. K, Krause T. W, Pulsed Eddy Current Detection of Cracks in Multilayer Aluminium Lap Joint, IEEE Sensor Journal, 15(2015), N°2, pp. 956-962.

[6] Xiao P., Tian S., Pei C., Yang G., Chen Z., Wang W., Wang W., Luo G., A Phased-Array EMAT for Detection of Delamination Defect in Tube of Multilayer Structure, Study in Applied Electrmagnetics and Mechanics, 41(2016), pp. 163-170.

[7] Bouali F., Yousfi G., Hamel M., Mohellebi H., Study of Physical and Geometrical Parameters Variation of NDT Device in Pulsed Eddy Current Using Coupled Circuit's Method, *International Conference of Modeling and Simulation* (2014), pp. 656-666. Algerie.

[8] Delage D., Ernst R., Prediction of the current distribution in an inductor with symmetry of revolution intended for heating by MF and HF induction, Revue Générale D'électricité (RGE), 1984, N°4, pp. 225-230.

[9] Maouche B., Alkama R., Feliachi M., Semi-analytical Calculation of the Impedance of a Differential Sensor for Eddy Current Non-Destructive Testing, *NDT& E International*, 42 (2009), N°7, pp. 573-580.

[10] Mohellebi H., Bouali F., Feliachi M., Use of Semi Analytical Method for the Detection of Defects in Diet Pulses, Serie Studies in Applied Electromagnetics and Mechanics, 35(2011), pp. 183-191.

[11] Akram Md. Sh. H., Terada Y., Keilchiro I., Kose K., Coupled Circuits numerical analysis of eddy currents in an open MRI, Journal of magnetic resonnace, 245 (2014), pp. 1-11.

[12] Bouzidi A, Maouche B., Feliachi M., Berthiau G., Pulsed eddy Current non Destructive Evaluation Based on coupled Electromagnetic Quantities, The European Physical Journal: Applied Physics, 57 (2012), pp. 1-9.

[13] Juillard J., Pichenot G., Mazia A., Semianalytical Méthod for Calculating the Impedance Variation for an Arbitrary Eddy-Current Probe, *IEEE. Transactions On Magnetics,* 38 (2002), N°5, pp. 3448 – 3453.

[14] Juillard J., De Barmon B., Berthiau G., A Simple Analytical three-dimensional Eddy Current Model, IEEE Transactions On Magnetics, 36 (2000), N°1, pp. 258-266.

[15] Pinda-Sanchez M., Roger-Folch J., Perez-Cruz J., Riera-Guasp M., Puche-Panadero R., Antonino-Daviu, Ponsllinares A., Calculation of Winding Inductances via Magnetic Vector Potential, Discrete Convolution and Fast Fourier Transform, PREZEGLAD ELECTROTECHNICZNY (Electrical Review), R. 86 NR 5/2010, ISSN: 0033-2097.

[16] Doirat V., Berthiau G., Fouladgar J., Olivier J. C., An Hybrid Analytical/E.C.C. Model Driven by Particle Swarm Optimization for Fibre Metal Laminates Testing, *Electromagnetic Non Destructive Evaluation* XII (2009), pp. 81-90.

[17] Gardiol F., *Traité électricité, Electromagnétisme,* Volume III, Presse Polytechniques et Universitaires Romandes, Suisse (1996).

[18] Martin J. Sablik, Robert E. Beissner, A. Choy, An Alternative Numerical Approach for Computing Eddy Currents: Case of the Doube-Layered Plate, *IEEE Transactions on Magnetics*, vol. MAG-20 (1984), N° 3, May 1984.